

See discussions, stats, and author profiles for this publication at: <https://www.researchgate.net/publication/245350268>

Vector Evaluated Particle Swarm Optimization (VEPSO) of Supersonic Ejector for Hydrogen Fuel Cells

Article in *Journal of Fuel Cell Science and Technology* · August 2010

DOI: 10.1115/1.4000676

CITATIONS

21

READS

191

2 authors:



Srisha M.V. Rao

Indian Institute of Science

76 PUBLICATIONS 448 CITATIONS

[SEE PROFILE](#)



Jagadeesh Gopalan

Indian Institute of Science

297 PUBLICATIONS 2,376 CITATIONS

[SEE PROFILE](#)

Some of the authors of this publication are also working on these related projects:



Effect of Duct Geometry on Mixing Characteristics in Constant Area Supersonic Ejector [View project](#)



Laser induced fluorescence [View project](#)

Vector Evaluated Particle Swarm Optimization (VEPSO) of Supersonic Ejector for Hydrogen Fuel Cell

Srisha Rao M V*

Department of Aerospace Engineering, IISc

G Jagadeesh †

Department of Aerospace Engineering

Indian Institute of Science

Banagalore, India PIN 560012

Abstract

Fuel cells are emerging as alternate green power producers, for both large power production as well as for use in automobiles. Hydrogen is seen as the best option as a fuel, however hydrogen fuel cells require recirculation of unspent hydrogen. Supersonic ejector is an apt device for recirculation in the operating regimes of a hydrogen fuel cell. Optimal ejectors have to be designed to achieve best performances. The use of Vector Evaluated Particle Swarm Optimization(VEPSO) technique to optimize supersonic ejectors with a focus on its application for hydrogen recirculation in fuel cells is presented here. Two parameters, compression ratio and efficiency have been identified as the objective functions to be optimized. Their relations to operating and design parameters of ejector is obtained by control volume based analysis using a constant area mixing approximation. The independent parameters considered are the area ratio and

*e-mail:srisharao@aero.iisc.ernet.in

†Corresponding author: Address: Department of Aerospace Engineering, Indian Institute of Science, Bangalore, Karnataka, PIN 560012, India; phone: +91-80-22933030; fax: +91-80-23606250; e-mail:jaggie@aero.iisc.ernet.in

the exit Mach number of the nozzle. The optimization is carried out at a particular entrainment ratio and results in a set of non-dominated solutions, the pareto front. A set of such curves can be used for choosing the optimal design parameters of the ejector.

Nomenclature

A	Area of cross-section [m^2]
AR	Characteristic area ratio of the ejector A_2/A_{1p}
CR	Compression ratio P_3/P_{os}
M	Mach number
P	Pressure [Pa]
\dot{m}	Mass flow rate [Kg/s]
T	Temperature [K]
X,X1,X2	Position vector of the swarm, 1 for swarm1 and 2 for swarm2
V,V1,V2	Velocity vector of the swarm
K	Control factor or weight for inertia effect in PSO
C_p	Control factor or weight for local effect in PSO
C_g	Control factor or weight for global effect in PSO
pbest	Personal best position of a swarm member
gbest	Global best position of the swarm
Greek	
ω	Mass flow ratio of secondary to primary fluid \dot{m}_s/\dot{m}_p
γ	Ratio of specific heats

η	Efficiency
τ	Stagnation temperature ratio T_{os}/T_{op}
α	Stagnation pressure ratio P_{os}/P_{op}

Subscripts

1, 2, ...	Stations or cross-sections in the ejector as shown in Figure 1
c	Station at which secondary fluid is aerodynamically choked
o	Stagnation property
s	Secondary or Entrained flow
p	Primary Flow

1 Introduction

In recent years there has been a rapid inflation in prices of fossil fuels and there is a growing concern on the longevity of the existing resources. The pollution generated by large power plants and automobiles have been a great cause of worry. All over the world there is a push towards greener alternatives to the conventional means of power production. Fuel cells have been identified as promising devices for generation of electricity in large scale as well as for transport applications. The Rolls-Royce Fuel Cell Systems have been developing such large power systems of capacities of about 1MW [1]. Leading automobile manufacturers realizing the capability of fuel cell driven vehicles are developing and testing Fuel Cell Vehicles (FCV) [2]. Direct hydrogen, or hydrogen derived from fuels like methanol or gasoline through chemical processing, or liquid fuels such as methanol are being studied for use in fuel cells. Hydrogen, having the highest calorific value, has tremendous potential as a fuel and is green

as well. Studies on relative total costs for various fuels show that a hydrogen based fuel cell system is best suited for automobile applications [3, 2]. It has been shown that with minor modifications to the existing structure of vehicles storage of hydrogen is feasible [3]. Besides the complexity of the vehicle is the least in case of a hydrogen fuel cell vehicle.

Hydrogen is always delivered in excess to the fuel cell stacks. Exhausting unspent hydrogen results in wastage of fuel and large fuel consumption. Unspent hydrogen needs to be recirculated for a low specific fuel consumption, which is a major bottleneck in hydrogen fuel cells. The unspent hydrogen after separation from the products of the reactions, firstly has to be mixed with fresh supply to meet the operating requirements of the fuel cell, and secondly being at lower pressure has to be pumped to the pressure of the fuel cell stacks. Supersonic ejector is a simple device that can perform both the functions. Ejectors are suitable devices for such applications. It uses the high pressure hydrogen stored in tanks to entrain the hydrogen for recirculation, mix the two flows and deliver it at the required pressure to the stacks[4]. Their advantage is that they require no external power, are simple in construction and have no moving parts. Ejectors find numerous applications, some of which are; in condenser vacuum system of steam power plants, ejector based refrigeration system[5, 6], thrust augmentation[7, 8], gas dynamic lasers[9]. Studies are being conducted for designing and testing ejectors as recirculation devices for Solid Oxide Fuel Cells [1, 10]. The use of ejectors as control devices ensuring a regulated mass flow into the fuel cell stacks is also being investigated [11, 12]. The possible use of ejectors to hydrogen fuel cell applications is a recent development. This paper focuses on the design of an optimized supersonic ejector for hydrogen recirculation using novel bio- inspired technique such as Vector Evaluated Particle

The flow within the ejector is complicated with shocks, expansions, mixing layers, boundary layers and their interactions. Despite extensive studies they are not understood fully. However the gross operation characteristics of ejectors have been studied experimentally as well as by using control volume methods for analysis. Keenan *et.al.* [13, 14] analyzed the overall flow through the ejector using control volume based methods. Such simplified methods are also used in sizing of ejectors for fuel cell systems [1, 10]. According to the conditions of mixing ejectors are classified as constant area ejector and constant pressure ejector [14]. It has been found that their trends are similar and do not deviate much from each other, so constant area analysis has been used as a base for evaluating performance of ejectors [15, 16]. There are three different regimes of operation of ejectors – supersonic, saturated-supersonic and the mixed regime [17, 18]. These three different regimes are distinguished by the phenomenon of the secondary flow choking which puts a limit on the mass flow that can be delivered by an ejector [19, 20]. Mixing, shocks and friction cause losses to the flow. These irreversibilities generate entropy and result in a reduction in the efficiency of the ejector [21]. Thus ejectors have lower thermodynamic efficiency as compared to turbomachinery, but their greatest advantage lies in their simplicity.

The major performance parameters of ejectors are the entrainment ratio (ω), the compression ratio (CR) and the efficiency η . They are influenced by stagnation pressure and temperatures of the two fluids, and geometry. Dutton and Carroll [15], have considered a single objective optimization of ejectors. Control volume analysis yields conflicting trends

for compression ratio and efficiency of the ejector, conditions favorable for improved efficiency reduce the compression ratio and vice versa. Thus optimizing the ejector for the best performance in terms of both compression ratio as well as efficiency is essential . Hence a multi-objective optimization of ejectors has been considered in this work. Two performance parameters, compression ratio and efficiency have been considered for optimization at a given entrainment ratio, which is a typical problem in recirculation systems. In general for a quasi 1D constant area analysis of ejectors,

$$CR = f(\alpha \tau M_{1p} AR \gamma \omega) \quad (1)$$

$$\eta = g(\alpha \tau M_{1p} AR \gamma \omega) \quad (2)$$

The relation of CR and η with other variables comes through the constant area ejector analysis. These equations though are algebraic in nature, have a lot of conditions like choking, and variables implicitly involved so that getting analytical results becomes difficult. Hence novel methods need to be used for optimization. Biologically inspired computing methods are finding extensive use nowadays to solve such multi-objective optimization problems. The modified Particle Swarm Optimization(PSO) technique, Vector Evaluated PSO(VEPSO) is used to accomplish the optimization[22, 23].

This study aims to

- Analyze ejectors for performance with hydrogen as the working fluid, using control volume based methods, constant area mixing.
- Identify design parameters and methods to achieve the required performance.

- Identify objective functions for optimization of ejectors.
- Carry out a multi-objective optimization to get relations for optimum ejector design.

2 Constant Area Ejector Analysis

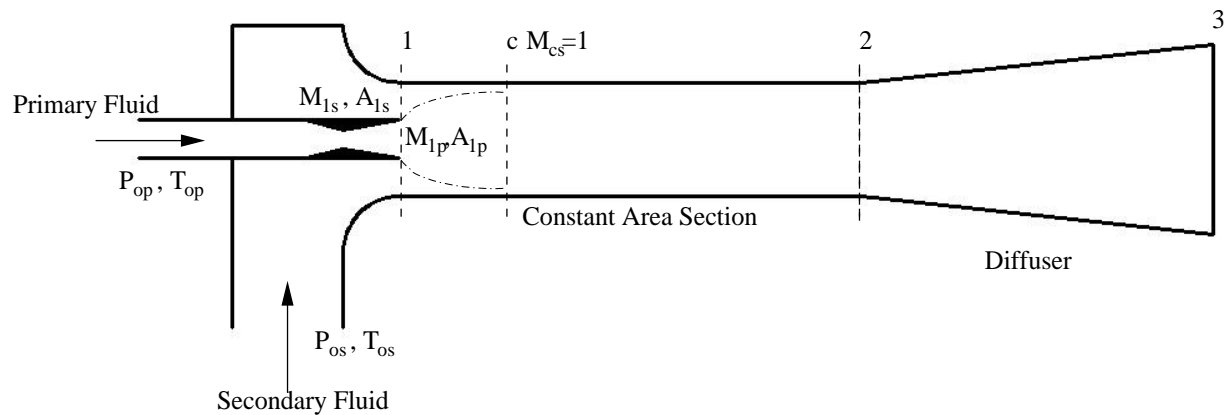


Figure 1: Schematic of a Constant Area ejector

A brief description of control volume analysis of the constant area ejector is given in this section, details of which can be found in references [14, 18, 24]. With reference to Figure 1, the schematic of a constant area ejector shows a supersonic nozzle within a constant area mixing duct followed by a subsonic divergent diffuser. Primary flow expands from high pressure through the supersonic nozzle into the constant area duct. The supersonic jet entrains the secondary fluid. Primary and secondary fluids mix in the constant area duct and

the resulting mixed flow can experience shock system within the duct whereby its velocity is reduced and pressure increased. The subsonic diffuser provides further pressure recovery.

The primary flow is choked at the throat of the supersonic nozzle, it is observed that for compression ratios less than a critical value the secondary flow is also choked and total mass flow through ejector becomes independent of the exit backpressure. Ejector operation is classified according to secondary flow choking [17, 18]. The ejector is said to operate in saturated-supersonic regime if the secondary flow is choked at the entrance to the constant area duct, section '1' in Figure1. An expanding jet creates a virtual converging duct for the secondary flow which results in secondary flow choking at cross-section 'c' in Figure 1. This is the aerodynamic choking phenomenon of secondary flows and this regime of operation of ejector is called supersonic regime. Under conditions such that secondary flow choking does not take place the ejector is operating in mixed regime where entrainment ratio is a strong function of compression ratio. For achieving maximum mass flow rate, ejectors are to be operated in either of the choked conditions. Thus the purpose of control volume analysis is to calculate the performance of ejector under choked flow conditions, which will yield parameters for optimization.

2.1 Assumptions

- a. The gas is taken to be calorically perfect.
- b. The primary and secondary flows are assumed to expand isentropically from their stagnation conditions to that of section '1'.

- c. The properties of the flow are piecewise uniform across cross-section ‘1’ and ‘c’, and completely uniform at all other cross-sections.
- d. The frictional effects of the walls are neglected.
- e. The shear layer between the two fluids between sections ‘1’ and ‘c’ is thin enough to assume that the flows are distinct.
- f. The flow is completely mixed and subsonic at section ‘2’.
- g. The flow in diffuser is isentropic.

2.2 Analysis

The control volume relations for constant area mixing appropriately simplified with the above assumptions lead to the following non dimensional forms of flow equations [24].

The Momentum Equation:

$$\left[\left(1 - \frac{G}{2}\right) \gamma^2 + \frac{G}{2} \gamma \right] M_2^4 + [(2 - G)\gamma] M_2^2 + 1 = 0 \quad (3)$$

where

$$G = \frac{\left[(1 + \gamma M_{1p}^2) + \gamma M_{1p}^2 \omega \left(\frac{V_{1s}}{V_{1p}} \right) \left(1 + \frac{1}{\gamma M_{1s}^2} \right) \right]^2}{\gamma M_{1p}^2 (1 + \omega) \left(1 + \left(\frac{\gamma-1}{2} \right) M_{1p}^2 \right) (1 + \omega \tau)} \quad (4)$$

and

$$\frac{V_{1s}}{V_{1p}} = \frac{M_{1s}}{M_{1p}} \sqrt{\tau \frac{1 + \frac{\gamma-1}{2} M_{1p}^2}{1 + \frac{\gamma-1}{2} M_{1s}^2}} \quad (5)$$

The Energy Equation:

$$\frac{T_{o2}}{T_{op}} = \frac{1 + \omega \tau}{1 + \omega} \quad (6)$$

The entrainment ratio is related to the geometry and operating conditions as in equation 7.

$$\omega = \frac{M_{1s}}{M_{1p}} \alpha (AR - 1) \sqrt{\frac{1}{\tau}} \left(\frac{1 + \frac{\gamma-1}{2} M_{1p}^2}{1 + \frac{\gamma-1}{2} M_{1s}^2} \right)^{\frac{\gamma+1}{2(\gamma-1)}} \quad (7)$$

In equations 3–7, The variables α , τ are operating parameters which are known or chosen. AR, the characteristic area ratio is the geometric parameter. M_{1p} , the exit Mach number of nozzle is known from nozzle geometry. Thus there are four unknowns: ω or AR, M_{1s} , M_m and T_{o2}/T_{op} and there are just three equations to solve for, equations 3, 6 and 7. The solution for M_{1s} has to be determined from the operating regime and the analysis for choking conditions.

2.2.1 Choking of secondary flow

When the ejector is operating in saturated-supersonic regime, where choking of secondary flow happens at section ‘1’, the conditions at section ‘1’ are given below.

$$M_{1s} = 1 \quad (8)$$

$$\frac{P_{1s}}{P_{1p}} \geq 1 \quad (9)$$

For supersonic regime, aerodynamic choking of secondary flow happens at section ‘c’. Control volume relations are set up between sections ‘1’ and ‘c’, considering primary and secondary flows to be distinct and the secondary flow attaining Mach number unity at ‘c’.

$$\frac{A_{1p}}{A_{cp}} = \frac{M_{cp}}{M_{1p}} \left(\frac{1 + \frac{\gamma-1}{2} M_{1p}^2}{1 + \frac{\gamma-1}{2} M_{cp}^2} \right)^{\frac{\gamma+1}{2(\gamma-1)}} \quad (10)$$

$$\frac{A_{1s}}{A_{cs}} = \frac{1}{M_{1s}} \left(\frac{2}{\gamma+1} \left(1 + \frac{\gamma-1}{2} M_{1s}^2 \right) \right)^{\frac{\gamma+1}{2(\gamma-1)}} \quad (11)$$

$$\frac{A_{1s}}{A_{cs}} = \frac{AR - 1}{AR - \frac{A_{cp}}{A_{1p}}} \quad (12)$$

$$\alpha(AR - 1)F(M_{1s}, \gamma) + F(M_{1p}, \gamma) = \alpha(AR - 1)\frac{A_{cs}}{A_{1s}}F(M_{cs}, \gamma) + \frac{A_{cp}}{A_{1p}}F(M_{cp}, \gamma) \quad (13)$$

where $F(M, \gamma)$ is defined as

$$F(M, \gamma) = \left[\frac{1 + \gamma M^2}{\left(1 + \frac{\gamma-1}{2} M^2\right)^{\frac{\gamma}{\gamma-1}}} \right] \quad (14)$$

Equations 10–13 are four equations to solve for four variables M_{1s} , M_{cp} , $\frac{A_{cp}}{A_{1p}}$ and $\frac{A_{cs}}{A_{1s}}$. The condition for supersonic choking is

$$M_{cs} = 1 \quad (15)$$

$$\frac{P_{1s}}{P_{1p}} < 1 \quad (16)$$

M_{1s} is evaluated, depending on the regime of choking, by using equation 8 or using equations 10-14. The M_{1s} is then used in equation 5.

The equation 3 is a quadratic for M_2^2 and will have valid solutions only if both the roots are real and positive. This pertains to a select region in the operating variable space. Of the two solutions for M_2 , one will be supersonic and other subsonic. Since the conditions of conservation of mass, momentum and energy are valid for a normal shock also, the solutions obtained in fact correspond to two sides of a normal shock. Whether a normal shock exists or not is decided by downstream pressure conditions. Here the flow at section ‘2’ is taken to be subsonic i.e. after a normal shock.

The pressure at section ‘2’ can be found using

$$\frac{P_2}{P_{1p}} = (1 + \omega) \frac{1}{AR} \frac{M_1}{M_2} \sqrt{\frac{T_{op}}{T_{o2}} \left(\frac{1 + \frac{\gamma-1}{2} M_m^2}{1 + \frac{\gamma-1}{2} M_{1p}^2} \right)} \quad (17)$$

Since the flow is adiabatic, the total enthalpy remains invariant, knowing M_2 and T_{o2} , T_2 can be easily calculated through isentropic relations.

2.2.2 Diffuser analysis

The flow within the diffuser is taken to be isentropic and the velocity at the exit of diffuser to be low enough for the static properties of the flow to be almost equal to the stagnation properties.

$$\frac{P_3}{P_2} = \left(1 + \frac{\gamma - 1}{2} M_2^2\right)^{\frac{\gamma}{\gamma-1}} \quad (18)$$

$$\frac{T_3}{T_2} = \left(1 + \frac{\gamma - 1}{2} M_2^2\right) \quad (19)$$

Hence the compression ratio of the ejector can now be evaluated

$$CR = \frac{P_3}{P_{os}} = \frac{P_3}{P_2} \frac{P_2}{P_{1p}} \frac{P_{1p}}{P_{op}} \frac{1}{\alpha} \quad (20)$$

2.2.3 Efficiency of ejector

The control volume equations give relations between the input and output flows of an ejector, thus a simple thermodynamic analysis of inlet and exit states of the ejector will yield the efficiency of the ejector. Since frictional forces are neglected in the preceding analysis, entropy generation is due to mixing and shock processes in the ejector which are irreversible [21].

The entropy generated in an ejector can be evaluated using equation 21

$$\frac{\Delta S_{ej}}{\dot{m}_p R} = \frac{\gamma}{\gamma - 1} \ln \frac{T_3^{(1+w)}}{T_{op} T_{os}^w} - \ln \frac{P_3^{(1+w)}}{P_{op} P_{os}^w} \quad (21)$$

A hypothetical isentropic process can be conceived that functions as an ideal ejector. The compression ratio of the hypothetical process can be evaluated by setting the left hand side of equation 21 to zero and solving for P_{3i}/P_{os} .

$$\frac{P_{3i}}{P_{os}} = \left(\tau^{-\frac{\omega}{\omega+1}} \left(\frac{1 + \omega \tau}{1 + \omega} \right) \right)^{\frac{\gamma}{\gamma-1}} (\alpha)^{\frac{1}{1+\omega}} \quad (22)$$

Taking the hypothetical ejector as a reference the efficiency of any ejector system can be defined as the ratio of the pressure increment of the secondary fluid in an actual ejector to that of the ideal one.

$$\eta = \frac{\frac{P_3}{P_{os}} - 1}{\frac{P_{3i}}{P_{os}} - 1} \quad (23)$$

The formulation presented in this section can be used for a gross analysis as well as design of ejectors. The calculated values show good agreement with experimental values [18]. In this paper the equations are solved for a fixed ω , τ with given fluid property γ . The variables are AR and M_{1p} . The performance parameters being solved for are CR and η , α also comes out as a solution. This implies that performance parameters are solved for different ejector geometries and operating conditions such that they give the prescribed ω .

Figure 2 plots efficiency vs compression ratio, for different ejectors with $\omega = 0.5$ and a

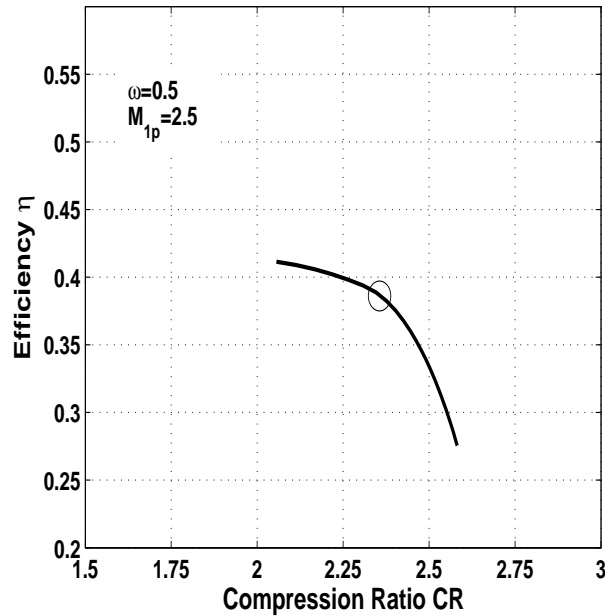


Figure 2: Plot for efficiency η vs Compression Ratio CR at $\omega = 0.5$

nozzle exit Mach number of 2.5. The ratio of specific heats is taken to be that of hydrogen, $\gamma = 1.41$ and the stagnation temperature ratio of the two fluids is taken to be unity. The plot shows that efficiency drops as compression ratio increases, at higher compression ratios efficiency is low and vice-versa. An optimal point would be a compromise between the two objective functions, i.e. as high a compression ratio as possible with good efficiency. From Figure 2 it can be seen that the efficiency drops slowly initially and the drop is sharp after the marked circular region. So the circular region marks the best conditions to operate the ejector for the given entrainment ratio and nozzle exit Mach number.

3 The Multi-Objective Optimization Problem

From Figure 2, it is clear that for a fixed entrainment ratio and a given nozzle Mach number, an optimal point exists. Hence for different nozzle exit Mach numbers such points can be identified and the best of the lot can be taken as the optimal design point for the given entrainment ratio. In this paper a procedure for optimization of two performance parameters, the compression ratio and the efficiency at a fixed entrainment ratio is described. This is the usual problem in designing ejectors to be used for recirculation purposes especially in fuel cell systems, where the recirculation mass flows are known and maximum pressure recovery at best efficiency is the goal. It is cumbersome to find the optimal point for every nozzle exit Mach number, hence an optimization procedure using the VEPSO principle is adopted which directly yields the plot of the optimal points called the pareto front. Of the influencing parameters, the area ratio and the exit Mach number of the nozzle are chosen to be independent parameters, and other parameters come out as solutions to the

constant area analysis. Since different combinations of the independent parameters can give optimum solutions, multi-objective optimization brings out a pareto front which is a set of non-dominated solutions[22].

A solution is said to be non-dominated if there are no other points better than it, which can be mathematically put as - If X be an element in a N -dimensional domain, $X = \{x_1, x_2, \dots, x_n\}$ having k objective functions $F(X) = \{f_1(X), f_2(X), \dots, f_k(X)\}$. For a case of maximization $F(Y)$ is said to weakly dominate $F(X)$ if

$$f_i(Y) \geq f_i(X) \forall i = 1, 2, \dots, k \quad (24)$$

i.e That the point Y at least does not deteriorate any of the objective functions than X and in some functions can be better than X . In this case $X = \left(M_{1p} \quad AR \right)$ and $F(X) = \left(\frac{P_3}{P_{os}} \quad \eta \right)$.

The constraints for the optimization problem are that $1.5 \leq M_{1p} \leq 3.5$, $1 \leq AR \leq 8$ [15]. There can be restrictions on the stagnation pressure ratio as well but is not taken in the present work. These kind of problems are tackled using search based algorithms which are inspired by optimization found in nature such as in natural selection, or in the behavior of social insects and animals.

4 The PSO Algorithm

The Particle Swarm Optimization(PSO) algorithm is a biologically inspired algorithm derived from flocking of birds[23]. Birds foraging for food over a large geographical area quickly converge upon not just any source but the one with abundance. This suggests some means

of communication which allow rapid exploration of the search area and convergence to the optimum. This behavior is mimicked in PSO algorithm. A brief description of this algorithm for single objective optimization and its extension to multi-objective case is given here [23, 22].

PSO is an iterative algorithm. Consider a single objective maximization, initially M particles of a swarm are randomly spread over an N -dimensional search space or domain. Every member of the swarm is associated with its position X , the velocity vector V and the value of the objective function F . Also each particle has a memory of the best position (pbest) that it has been to among all iterations until then and the whole swarm has a store of the global best it has encountered (gbest). At each iteration the value of objective function F is evaluated for each particle at its position X_i . This value is compared with pbest and if it is greater pbest is changed to the present value else it is left unchanged. Similarly the whole swarm is scanned for the gbest. The update for the next iteration is done using equations 25 and 26.

$$V_{i+1}^j = KV_i^j + C_p r_1 (pbest_i^j - X_i^j) + C_g r_2 (gbest_i - X_i^j) \quad (25)$$

$$X_{i+1}^j = X_i^j + V_{i+1}^j \quad (26)$$

Thus a particle is influenced by its self inertia through V_i , its position relative to pbest and gbest. Inertia tends to let the particle wander in the search space, while pbest and gbest gives a direction for the search. The relative influence of these effects is controlled through the parameters K , C_p and C_g , which ensure both a proper exploration of the domain as well as fast convergence to the optimum.

4.1 The VEPSO Algorithm

The Vector Evaluate PSO algorithm is an adaptation of the PSO algorithm to solve for multi-objective optimization problems [22]. There are as many swarms as objective functions. Each swarm executes a PSO separately for its objective function, but an inter-swarm communication is set up so that the optimum position of each swarm is made available to other swarms so that they adjust themselves accordingly. This is best explained through two objective function optimization which is also what is being presented here.

Two swarms of equal population are considered here. Swarm1 is associated with compression ratio(CR)as its objective function and swarm2 with efficiency(η). Each swarm is evaluated separately following the PSO algorithm. The pbest for every member of each swarm ($pbest1^j$ and $pbest2^j$) and the gbest ($gbest1$ and $gbest2$) is evaluated. The gbest of one swarm is passed into the other for updatation i.e, in equation 25, the gbest for swarm1 will be gbest2 and in swarm2 gbest1.

$$V1_{i+1}^j = KV1_i^j + C_p r_1 (pbest1_i^j - X1_i^j) + C_g r_2 (gbest2_i - X1_i^j) \quad (27)$$

$$X1_{i+1}^j = X1_i^j + V1_{i+1}^j \quad (28)$$

$$V2_{i+1}^j = KV2_i^j + C_p r_1 (pbest2_i^j - X1_i^j) + C_g r_2 (gbest1_i - X2_i^j) \quad (29)$$

$$X2_{i+1}^j = X2_i^j + V2_{i+1}^j \quad (30)$$

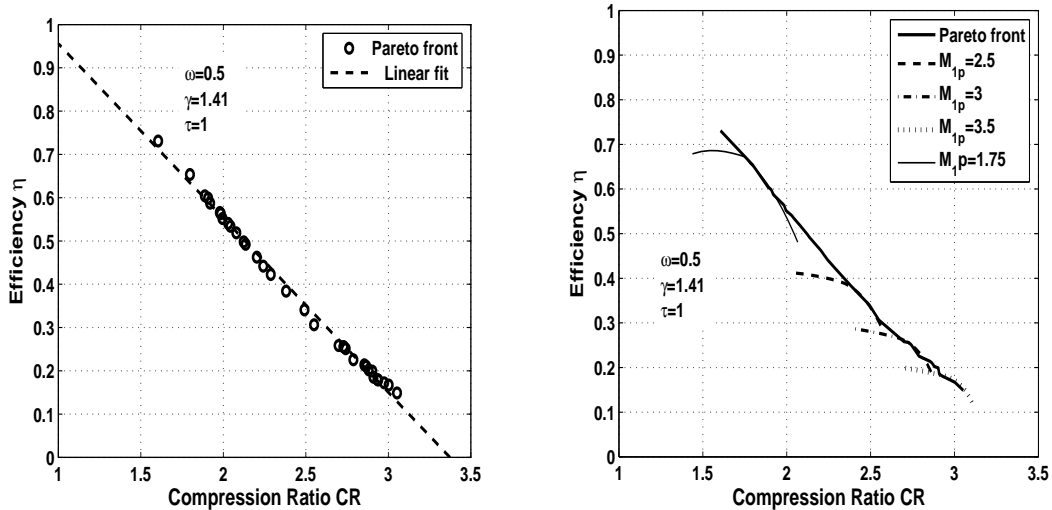
4.1.1 Algorithm

To solve for the optimum points or the pareto front the following procedure is adopted.

- i. The input for a required entrainment ratio, stagnation temperature ratio of the operation

and the γ of the fluid is taken.

- ii. The limits of AR and M_{1p} are set.
- iii. Two swarms, swarm1 and swarm2 are initialized with random values of AR and M_{1p} .
- iv. For each of the two swarms.
 - a. For every member in the swarm perform constant area calculations to get the performance parameters CR and η .
 - b. Check whether the results are valid if not the value of AR and M_{1p} are changed until valid results are obtained.
 - c. Evaluate pbest. Swarm1 is evaluated for CR and swarm2 for η .
 - d. Evaluate gbest; gbest1 is evaluated by comparing CR and gbest2 by comparing η .
 - e. Update each swarm by using the gbest of the other swarm using equations 27–30.
 - f. Check if the updated values are within the limits set, if not reset them within the limits.
- v. This is iteratively continued until maximum number of iterations, or until gbest values stagnate for both the swarms for a certain number of iterations.
- vi. The resulting swarms from the procedure are searched for the non-dominating solutions based on equation 24, which are picked to get the pareto front.



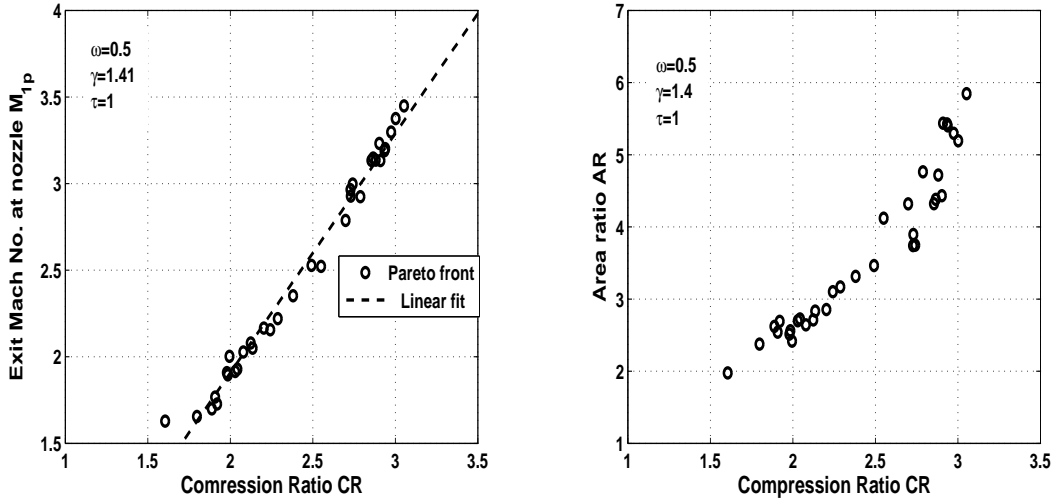
(a) Efficiency (η) vs Compression Ratio (CR) (b) Comparison with plots for certain M_{1p}

Figure 3: The Pareto Front

5 Results and Discussions

The VEPSO algorithm is run with the following conditions, fluid-Hydrogen ($\gamma = 1.41$), $\omega = 0.5$, $\tau = 1$. The control parameters of PSO are taken as $K = 0.4$, $C_p = 0.02$, $C_g = 0.02$. Maximum number of iterations is set to 1000 and the code terminates if the value of gbest of both the swarms do not change for 300 successive iterations. The population of each swarm is 20.

The plot in Figure 3(a) shows the pareto front, i.e. the set of non-dominated solutions for an entrainment ratio of 0.5, which is linear. In order to ascertain that the algorithm has indeed picked up the right optimal points, the plots of η vs CR for a few Mach numbers (similar to what has been plotted in Figure 2) have been plotted along with the Pareto front in Figure 3(b). It can be seen that the Pareto front got by VEPSO algorithm does pick up the optimal regions of every Mach number plot. It turns out that the Pareto front is linear



(a) The Mach number at exit of the nozzle

(b) The Area Ratio

Figure 4: The optimal design parameters

with a negative slope reflecting the trend that compression ratio and efficiency oppose each other. So a single optimal point cannot be prescribed (for which the pareto front has to be nonlinear with a maxima), however the line does represent the best operating points for an ejector with entrainment ratio 0.5. If a particular compression ratio is to be achieved then the maximum possible efficiency for which an ejector can be designed will be a point on the line. And the pareto front gives all such possible solutions, for every CR achievable within the constraints set for the independent variables.

The design parameters corresponding to the pareto solutions are plotted with respect to CR in Figures 4(a)& 4(b). Figure 4(a) gives the plot of Mach number at exit of the nozzle M_{1p} and Figure 4(b) the characteristic area ratio AR. Once the required CR is chosen, the design parameters can be directly read off from these graphs, which almost fixes the quasi 1D design of the constant area ejector. The optimal conditions at which the ejector has to

be operated so as to obtain entrainment ratio of 0.5 also comes out as part of optimization. Since the stagnation temperature ratio of the two fluids τ is fixed, the stagnation pressure ratio α that has to be provided, is plotted vs CR in Figure 5

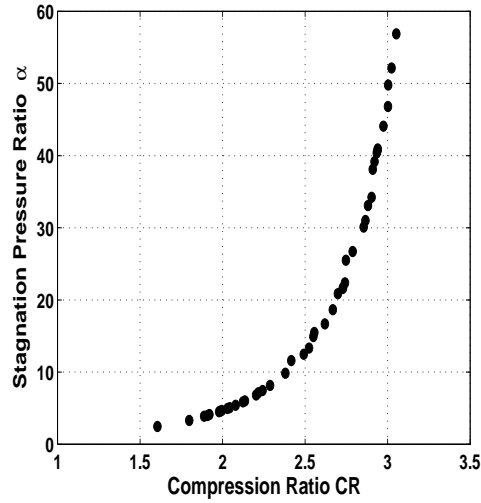


Figure 5: Stagnation Pressure ratio of secondary and primary fluids at section ‘1’, α

The stagnation pressure ratio is indicative of the primary pressures that need to be provided for achieving compression ratio. It can be seen to increase slowly in the beginning but later the increase is very rapid. This is also because of strong shocks that occur at higher compression ratios requiring greater primary flow momentum and energy hence higher stagnation pressures. No restrictions on the stagnation pressure ratio has been imposed in the optimization done here, but it can be taken care of explicitly. In case the stagnation pressure ratio is limited by other constraints (such as supply pressure and storage constraints) then the optimal compression ratio can in turn be determined. For most of pareto points the Mach number of the secondary flow at the entrance to the ejector is found to lie between 0.7 and 0.8. For example an optimal ejector giving an entrainment ratio of 0.5 and $CR = 2.5$

will give from the graphs, $M_{1p} = 2.6$, $AR = 3.5$ and $\alpha = 12.5$. The results for only an entrainment ratio of 0.5 have been presented here, the same procedure can be repeated for any entrainment ratio for which the ejector needs to be designed and similar plots can be obtained which will help in design of optimal ejectors.

Larger Mach number of the primary flow results in higher compression ratios because of larger momentum flux, however the strength of the shock being much higher results in decrease of efficiency. Larger area ratios allow the primary flow to expand to higher Mach numbers before secondary choking results, again leading to stronger shocks after mixing. While small area ratios results in the secondary getting choked at the entrance itself, and such flows can support only a lower compression ratio. Thus the pareto points are such that the combinations of area ratio and exit Mach number of the nozzle are optimal to allow good momentum augmentation yet the shock strengths do not bring down the efficiency much.

Runs on other entrainment ratios showed that the trends are similar to what has been presented here. It is observed that at higher entrainment ratios the compression ratio achievable by the optimal ejector decreases rapidly. Higher entrainment ratios imply larger mass flow rates of secondary flow driven by smaller mass flows of primary flow, hence the momentum augmentation decreases consequently there is a decrease in the compression ratios that can be achieved. It is also seen that the choking regime moves over to the saturated supersonic regime where the secondary flow chokes at the entry to the constant area duct. This is again a consequence of larger secondary mass flows.

In the present analysis losses due to friction and shear have not been taken care of so the efficiency that is calculated is only indicative of ejector's actual efficiency which will be lower than the one obtained. Since the major losses in the ejector are due to shocks and mixing the trends can be expected to be similar. If the frictional effects are also taken into consideration, then the length of the ejector will be an additional independent parameter. The optimization procedure described here is quite general and can also be carried out in conjunction with CFD where the exact geometry of the ejector itself can be optimized for. However for a first cut design control volume relations with VEPSO optimization can be used.

6 Conclusions

Supersonic ejectors are simple devices that can be used for recirculation of hydrogen fuel in a fuel cell system. Ejectors need to be optimized for best performance. Control volume method serves as simple model for the ejector which can be solved to get the gross flow properties across it. Thus the functional relation between the performance parameters and design variables can be evaluated which yield the trends for optimizing the ejector. The usefulness of VEPSO based multi-objective optimization algorithm to arrive at optimum values for design parameters of an ejector has been demonstrated. The ejector is optimized for compression ratio and efficiency at a particular entrainment ratio, typical to recirculation of fuels as hydrogen in fuel cells, with characteristic area ratio and Mach number at exit of the nozzle as design variables. No restriction is laid on the stagnation pressure ratio of the two flows. The optimization procedure results in a pareto front which is a curve in the objective

function space denoting a set of non-dominated solutions. Plots of the design variables at the pareto points can then be plotted. A particular operating point can be chosen from this set and the corresponding design parameters used for sizing an ejector can be inferred. At the optimal points the combination of area ratio and exit Mach number of the nozzle are such that a good momentum augmentation to the secondary flow happens without generating very strong shocks to cause much decrease in the efficiency of the ejector. A typical example of an ejector delivering an entrainment ratio of 0.5 is illustrated.

References

- [1] Ferrari, M. L., Bernardi, D., and Massardo, A. F., 2006, “Design and testing of ejectors for high temperature fuel cell hybrid systems,” *Journal of Fuel Cell Science and Technology*, Trans. ASME, **3**, pp. 284–291.
- [2] Shukla, A. K., Jackson, C. L., and Scott, K., 2003, “The promise of fuel cell-based automobiles,” *Bulletin of Materials Science*, **26 No.2**, pp. 207–214.
- [3] Thomas, C., James, B. D., Jr, F. D. L., and Jr, I. F. K., 2000, “Fuel options for the fuel cell vehicle: hydrogen, methanol or gasoline?” *International Journal of Hydrogen Energy*, **25**, pp. 551–567.
- [4] Lee, J.-H., Sameen, A., Kumar, V. S., and Kim., H., 2005, “Studies on ejector systems for hydrogen fuel cell,” *41st Jt. Propulsion conference*.
- [5] Chunnanond, K. and Aphornratana, S., 2004, “Ejectors: applications in refrigeration technology,” *Renewable and Sustainable Energy Reviews*, **8**, pp. 129–155.

- [6] Huang, B., Jiang, C., and Hu, F., 1985, "Ejector performance characteristics and design analysis of jet refrigeration system," *Journal of Fluids Engineering, Trans. ASME*, **107**, pp. 792–802.
- [7] Alperin, M. and Wu, J.-J., 1983, "Thrust augmenting ejectors part I," *AIAA Journal*, **21**(10), pp. 1428–1436.
- [8] Alperin, M. and Wu, J.-J., 1983, "Thrust augmenting ejectors part II," *AIAA Journal*, **21**(12), pp. 1698–1706.
- [9] Dutton, J., Mikkelsen, C., and Addy, A., 1982, "A theoretical and experimental investigation of the constant area, supersonic-supersonic ejector," *AIAA Journal*, **20**(10), pp. 1392–1400.
- [10] Zhua, Y., Cai, W., Wen, C., and b, Y. L., 2007, "Fuel ejector design and simulation model for anodic recirculation soft system," *Journal of Power Sources*, **173**, p. 437449.
- [11] Karnik, A. Y., Sun, J., and Buckland, J. H., 2006, "Control analysis of an ejector based fuel cell anode recirculation system," *Proceedings of the 2006 American Control Conference Minneapolis, Minnesota*, pp. pp. 1942–1948.
- [12] Ferrari, M. L., Traverso, A., Magistri, L., and Massardo, A. F., 2005, "Influence of the anodic recirculation transient behaviour on the soft hybrid system performance," *Journal of Power Sources*, **149**, p. 2232.
- [13] Keenan, J. and Neumann, E., 1942, "A simple air ejector," *Journal Of Applied Mechanics*, pp. A-75–A-81.

- [14] Keenan, J., Neumann, E., and Lustwerk, F., 1950, “An investigation of ejector design by analysis and experiment,” *Journal Of Applied Mechanics*, pp. 299–309.
- [15] Dutton, J. and Carroll, B., 1986, “Optimal supersonic ejector designs,” *Journal of Fluids Engineering, Trans. ASME*, **108**, pp. 414–420.
- [16] J.Fabri and J.Paulon, 1958, *Theory and Experiment on Supersonic Air-to-Air Ejectors*, NACA.
- [17] Chow, W. and Addy, A., 1964, “Interaction between primary and secondary streams of supersonic ejector systems and their performance characteristics,” *AIAA Journal*, **2**(4), pp. 686–695.
- [18] Addy, A., Dutton, J., and Mikkelsen, C., 1981, *Supersonic Ejector-Diffuser Theory and Experiment*, University of Illinois Urbana.
- [19] Munday and Bagster, “A new ejector theory applied to a steam jet refrigeration,” *Ind. Eng. Chemistry Process And Design*, **16**(4).
- [20] Chou, S., Yang, P., and Yap, C., 2001, “Maximum mass flow ratio due to secondary flow choking in an ejector refrigeration system,” *International Journal of Refrigeration*, **21**(10), pp. 486–499.
- [21] Arbel, A., Shkiyar, A., Hershgal, and et.al., 2003, “Ejector irreversibility characteristic,” *Journal of Fluids Engineering, Trans. ASME*, **125**, pp. 121–129.

- [22] Omkar, S., Mudigere, D., Naik, G. N., and Gopalakrishnan, S., 2008, “Vector evaluated particle swarm optimization (vepso) for multi-objective design optimization of composite structures,” *Computers and Structures*, **86**, p. 114.
- [23] Kennedy, J. and Eberhart, R. C., 1995, “Particle swarm optimization,” *Proceedings of IEEE International Conference on Neural Networks, Piscataway, NJ.*, pp. pp. 1942–1948.
- [24] Chant, L. J. D., 2003, “Subsonic ejector nozzle limiting flow conditions,” *Journal of Engineering for Gas Turbines and Power*, **125**, pp. 851–854.

List of Figure Captions

1. Figure 1: Schematic of a Constant Area ejector
2. Figure 2: Plot for efficiency vs CR at $\omega = 0.5$
3. Figure 3: Efficiency η vs Compression Ratio CR
4. Figure 4: Comparison with plots for certain M_{1p}
5. Figure 5: The Mach number at exit of the nozzle
6. Figure 6: The Area Ratio
7. Figure 7: Stagnation Pressure ratio of secondary and primary fluids at section '1', α